HHS Public Access

Author manuscript

Exp Eye Res. Author manuscript; available in PMC 2018 December 01.

Published in final edited form as:

Exp Eye Res. 2017 December ; 165: 20–28. doi:10.1016/j.exer.2017.08.018.

Contrasting Cellular Damage After Blue-IRIS and Femto-LASIK in Cat Cornea

Kaitlin T. Wozniak[1,§], **Noah Elkins**[2,§], **Daniel R. Brooks**[1], **Daniel E. Savage**[1,3,4], **Scott MacRae**[3,4], **Jonathan D. Ellis**[1,5], **Wayne H. Knox**[1,3], and **Krystel R. Huxlin**[3,4,*]

[1]The Institute of Optics, University of Rochester, Rochester, NY 14627, USA

[2]Department of Biomedical Engineering, University of Rochester, Rochester, NY 14627, USA

[3]Center for Visual Science, University of Rochester, Rochester, NY 14627, USA

[4]Flaum Eye Institute, University of Rochester, Rochester, NY 14627, USA

[5]Department of Mechanical Engineering, University of Rochester, Rochester, NY 14627, USA

Abstract

Blue-intra-tissue refractive index shaping (Blue-IRIS) is a new approach to laser refractive correction of optical aberrations in the eye, which alters the refractive index of the cornea rather than changing its shape. Before it can be implemented in humans, it is critical to establish whether and to what extent, Blue-IRIS damages the cornea. Here, we contrasted the impact of −1.5 D cylinder refractive corrections inscribed using either Blue-IRIS or femtosecond laser *in situ* keratomileusis (femto-LASIK) on corneal cell viability. Blue-IRIS was used to write a −1.5 D cylinder gradient index (GRIN) lens over a 2.5 mm by 2.5 mm area into the mid-stromal region of the cornea in six freshly-enucleated feline eyes. The same correction (−1.5 D cylinder) was inscribed into another four cat eyes using femto-LASIK. Six hours later, all corneas were processed for histology and stained for terminal deoxynucleotidyl transferase-mediated dUTP35 digoxigenin nick end labeling (TUNEL) and p-γ-H2AX to label damaged cells. In Blue-IRIS-treated corneas, no tissue was removed and TUNEL-stained cells were confined to the laser focal zone in the stroma. In femto-LASIK, photoablation removed 14 μm of anterior stroma, but in addition, TUNEL-positive cells clustered across the femto-flap, the epithelium at the flap edges and the stroma below the ablation zone. Keratocytes positive for p-γ-H2AX were seen adjacent to all Blue-IRIS focal zones, but were completely absent from femto-LASIK-treated corneas. Unlike femto-LASIK, Blue-IRIS attains refractive correction in the cornea without tissue removal and only causes minimal, localized keratocyte death within the laser focal zones. In addition, Blue-

Correspondence and reprint request: Krystel R. Huxlin, PhD, University of Rochester Eye Institute, 601 Elmwood Ave, Box 314, Rochester, NY 14642, USA; Phone +1-(585) 275-5495; huxlin@cvs.rochester.edu.

[§]Equal first authors

The authors declare the following interests: K.R. Huxlin, W. H. Knox, and J. D. Ellis have founder's equity in Clerio Vision, Inc., which partially supported this research. K. R. Huxlin, W. H. Knox, and J. D. Ellis have no fiduciary responsibility in Clerio Vision, Inc.

IRIS induced DNA modifications associated with phosphorylation of γ-H2AX in keratocytes *adjacent* to the laser focal zones. We posit that this p-γ-H2AX response is related to alterations in chromatin structure caused by localized changes in osmolarity, a possible mechanism for the induced refractive index changes.

Keywords

refractive correction; stroma; refractive index modification; GRIN lens; photoablation; TUNEL; γ-H2AX

1 Introduction

The wound healing response that follows tissue removal in laser refractive procedures such as laser *in-situ* keratomileusis (LASIK) and photorefractive keratectomy (PRK) has been studied extensively and appears to underlie at least some of the post-operative complications observed following these procedures (Fan-Paul *et al.*, 2002; Mohan *et al.*, 2003; Netto *et al.*, 2005; Wilson, 1997, 2000; Wilson and Kim, 1998). These complications include stromal haze, induction of higher order aberrations, patient discomfort, and dry eye (Lee *et al.*, 2005; Campos *et al.*, 1994; Netto *et al.*, 2007; Ambrósio *et al.*, 2008; Netto *et al.*, 2005). Nakamura *et al.* stated in 2001 that an intact epithelial-stromal interaction is essential to avoid stromal haze (Nakamura *et al.*, 2001). Cell death can also contribute to these complications because it triggers a series of changes that both induce and potentiate wound healing (Helena *et al.*, 1998; Meltendorf *et al.*, 2007; Netto *et al.*, 2005; Wilson, 1997, 2000; Wilson and Kim, 1998). Thus, if tissue damage could be reduced, the detrimental effects of laser refractive corrections may decrease.

In 2010, building on previous work in which refractive index change was observed in ophthalmic hydrogels (Ding *et al.*, 2006; Ding *et al.*, 2009), we proposed a new method for refractive correction that did not involve tissue removal. Hydrogels have been, and continue to be used as tissue substitutes for development of the IRIS procedure as they can be shaped into cornea-like structures with similar thickness, transparency and hydration. Once reproducible IRIS patterns were inscribed in hydrogels, we translated the procedure to cornea and using a high-repetition rate, 400 nm femtosecond laser, with intensities below the damage threshold of the cornea, we were able to locally modify the refractive index (RI) of the corneal matrix (Ding *et al.*, 2008; Nagy *et al.*, 2010; Xu *et al.*, 2010; Xu *et al.*, 2011a) – an approach termed Blue-Intra-tissue Refractive Index Shaping (Blue-IRIS). We subsequently showed that Blue-IRIS could be used to alter corneal refractive power *in vivo* (Savage *et al.*, 2014). The native two-photon absorption of the cornea at 400 nm, coupled with a high numerical aperture (NA) laser delivery system, created a highly localized region of refractive index (RI) change (Xu *et al.*, 2010; Xu *et al.*, 2011b). By translating this focal region through the cornea, it was possible to inscribe one to three closely-spaced, identically-written, custom gradient index (GRIN) layers and attain significant changes in refractive power (Brooks *et al.*, 2014; Savage *et al.*, 2014). We hypothesized that because Blue-IRIS did not require epithelial debridement, flap creation, or tissue removal, it should prove less invasive and damaging to the cornea than traditional laser refractive surgeries

(Campos *et al.*, 1994; Møller-Pedersen *et al.*, 2000; Nakamura *et al.*, 2001; Netto *et al.*, 2007).

Here, we tested this hypothesis by contrasting the amount of cellular damage that occurs following Blue-IRIS in living cornea with damage induced by femto-LASIK designed to generate an identical amount of refractive correction: a −1.5 D cylinder change. This correction was chosen to mirror previous IRIS refractive corrections performed in live cats (Savage *et al.*, 2014), thus providing an opportunity to study the biological consequences of those corrections. We chose to also study femto-LASIK because, like Blue-IRIS, this procedure uses a femtosecond laser. However, unlike Blue-IRIS, femto-LASIK causes photo-disruption to create a corneal flap. Once the flap is lifted, an excimer laser ablates the stromal bed to generate refractive change.

Cell damage was assayed using terminal deoxynucleotidyl transferase-mediated dUTP-digoxigenin nick end labeling (TUNEL) assay, and antibodies to the phosphorylated form of γ-H2AX (p-γ-H2AX). While the TUNEL assay is a popular tool for identifying dying cells (Gavrieli *et al.*, 1992; Wilson, 2000; Wilson *et al.*, 1996), the implications of positive p-γ-H2AX staining are less clear. The latter has been used both as a marker for DNA damage and changes in chromatin structure that did not lead to cell death (Baure *et al.*, 2009; Clingen *et al.*, 2008; Jester *et al.*, 2012; Kuo and Yang, 2008; Mah *et al.*, 2010; Van Attikum and Gasser, 2009; Vogel *et al.*, 2005). Given that Blue-IRIS does not remove corneal tissue, a detailed examination of multiple forms of DNA damage in all corneal layers is an important first step for gauging the safety and potential for post-operative complications of this new procedure.

2 Methods

2.1 Blue-IRIS Instrumentation and Procedure

The femtosecond laser system used to perform Blue-IRIS (Fig. 1) was identical to that described in our previous publications (Brooks *et al.*, 2014; Savage *et al.*, 2014). In brief, we used a mode-locked Ti:Sapphire oscillator (Vitesse; Coherent Corporation, Santa Clara, CA) emitting 800 nm, 100 fs pulses at 80 MHz. A second-harmonic generator frequency-doubled the laser pulses, producing approximately 250 mW of 400 nm femtosecond pulses. During Blue-IRIS, the pulses were focused into the corneal stroma via a 1.0 NA water-immersion objective (20X, W Plan-Apochoromat, Carl Zeiss, Jena, Germany). A metallic, variable neutral density filter was used to adjust the average beam intensity to 60±1 mW, which corresponds to pulse energies on the order of 0.8 nJ. During Blue-IRIS, the cornea remained stationary and applanated while the laser delivery system scanned across it in the x-and y-directions. The objective was mounted to a commercial vibration exciter (Measurement Exciter Type 4810; Brüel & Kjær, Nærum, Denmark), which, in turn, was mounted to a vertical-translation stage (GTS30V; Newport Corporation, Irvine, CA) on top of a linear translation stage (GTS70; Newport Corporation, Irvine, CA). The vibration exciter, in conjunction with the linear stage, provided for a raster scan motion while the vertical stage controlled the depth of the focal region in the stroma. The resulting pattern of RI change occupied an en-face area ~2.5 mm by 2.5 mm, consisting of 1 μm center-spaced lines written into the mid to anterior stroma (Brooks *et al.*, 2014; Savage *et al.*, 2014).

Six feline eyeballs were obtained post-mortem from domestic short hair cats (*felis cattus*) by an approved supplier (Liberty Research Inc., Waverly, NY). The globes were removed from the animals immediately after euthanasia; they were immersed in Optisol-GS (Bausch & Lomb Inc., Rochester, NY) and shipped to our laboratory overnight on ice. All animal procedures were conducted in accordance with guidelines of the University of Rochester Committee on Animal Research, the ARVO statement for the Use of Animals in Ophthalmic and Vision Research, and the NIH Guide for the Care and Use of Laboratory Animals. Upon arrival, Blue-IRIS was performed as follows: each globe was secured inside a foam cup using holding pins (Fig. 2A). Applanation of the cornea was achieved using a custom-built, polycarbonate suction ring with a 10 mm diameter opening and a 170-μm-thick histology-grade glass coverslip. A flat-edged needle inserted into the side of the polycarbonate ring provided suction, applanating the cornea as previously described (Savage *et al.*, 2014). In two of the corneas, three identical, square (2.5×2.5 mm) GRIN patterns (Fig. 2B) were successively inscribed parallel to the applanator, 10 μm apart, ~150 μm below the epithelium. In the remaining four corneas, GRIN layers were more widely spaced (~30 μm), starting ~100 μm below the epithelium (Fig. 2C). In all cases, the overall refractive structure created by these GRIN lenses was identical to that previously shown to induce −1 to −1.5 D of cylinder (Savage *et al.*, 2014).

2.2 Femto-LASIK Procedure

Four feline eyeballs underwent femto-LASIK as follows: an 8.5 mm flap was cut using the Femto LDV (Zeimer Ophthalmic Systems, Port, Switzerland) at an intended depth of ~100 μm below the epithelium. The flap was pulled back to expose the stroma, which underwent a −1.5 D cylinder ablation over a 4 mm optical zone, (the smallest optical zone that could be created by our system) surrounded by a transition zone, in the center of the cornea, using a Technolas 217 laser (Bausch & Lomb Inc., Rochester, NY). The Technolas 217 laser operates at 193 nm, with a pulse frequency of 100 Hz, and a pulse duration of ~18 ns. Post-ablation, the flap was replaced over the stromal bed until secure.

2.3 Tissue Processing for Histology

Following Blue-IRIS and femto-LASIK, a 2–3 mm long penetrating incision was made in the far periphery of each cornea to serve as a positive [wound] control for TUNEL staining. The globes were then placed back into Optisol-GS (Bausch & Lomb, Inc., Rochester, NY) for 6 hours to allow for the DNA degradation typical of cell death (and necessary for TUNEL staining) to occur (Wilson and Kim, 1998). At the end of this period, globes were immersion-fixed in 4% paraformaldehyde in cold, 0.1 M Phosphate Buffered Saline (PBS; pH 7.4) for 12 to 16 hours before cryo-protection in 30% sucrose in 0.1 M PBS at 4 °C for another 24 hours. Finally, corneas were dissected around the scleral rim, mounted in OCT Compound (Tissue Tek; Sakura Finetek, Torance, CA), frozen and sectioned into 20 μm-thick slices using a cryostat (2800 Frigocut E; Leica, Bannockburn, IL). Individual sections were mounted on gelatin-coated microscope slides for staining.

TUNEL staining was performed using the ApopTag® Red *In Situ* Apoptosis Detection Kit (S7165, Chemicon International, Millipore Inc., Temecula, CA). Slide-mounted corneal sections were first dried and rinsed in 0.1 M PBS before being post-fixed in pre-cooled

ethanol:acetic acid 2:1 for 5 minutes at −20 °C. The sections were then rinsed and incubated at room temperature with equilibration buffer, followed by terminal deoxynucleotidyl transferase enzyme for 1 hour in a humidified chamber. The reaction was halted with stop/wash buffer applied for 10 minutes followed by another wash in PBS. Warmed rhodamine-labeled, anti-digoxigenin was applied to the sections and incubated in a dark, humidified chamber for 30 min. After a final rinse in PBS, the stained sections were cover-slipped with mounting medium containing DAPI (VECTASHIELD®; Vector Laboratories, Burlingame, CA).

Immuno-staining for p-γ-H2AX was performed on adjacent slides and sections to those used for TUNEL staining. Corneal sections were incubated with a mouse monoclonal anti-γ-H2AX (phosphor S139) antibody (clone 9F3, Cat. #AB26350; Abcam, Cambridge, MA) diluted at 1:500 in 0.1M PBS containing Triton X 100 for ~16 hours. After rinsing the tissue with PBS, a secondary antibody, Alexa-Fluor-555 conjugated to goat anti-mouse IgG (Cat. #A21422; Invitrogen; Grand Island, NY) diluted 1:400 with the same diluent as the first antibody, was applied to the sections at room temperature for two hours. After a final rinse in PBS, sections were counterstained and cover-slipped with mounting medium containing DAPI (VECTASHIELD®; Vector Laboratories, Burlingame, CA).

All stained sections were imaged using an AX70 Olympus Microscope (Olympus Corporation, Tokyo, Japan). Photomicrographs were obtained using a high-resolution Microfire digital camera interfaced with a computer running the Q-Capture Pro 7 software (QImaging, Surrey, BC, Canada). Blue-IRIS layers and the femtosecond flap cuts auto-fluoresced green under 488 nm excitation; p-γ-H2AX-and TUNEL-positive cells fluoresced red under rhodamine illumination; DAPI-positive cells fluoresced blue under 350 nm illumination.

2.4 Cell Counting and Analysis

Using a 10× microscope objective, we first acquired photomicrographs of sequential, adjacent, non-overlapping, corneal regions labeled for either TUNEL/DAPI or p-γ-H2AX/DAPI and extending the entire length of the inscribed Blue-IRIS or femto-LASIK interventions, including the 8.5 mm femto-flap (e.g. Figs. 3–5). For each corneal location of interest, images were taken under 488 nm, 550 nm, and 350 nm illumination to visualize the Blue-IRIS pattern, TUNEL or p-γ-H2AX cells, and DAPI positive cells, respectively. Corresponding image triplets were merged using Adobe Photoshop CS (Adobe Systems Inc., San Jose, CA).

Six sections stained with TUNEL/DAPI were analyzed from corneas with tightly spaced Blue-IRIS patterns, and five TUNEL/DAPI-stained sections were analyzed for corneas inscribed with loosely spaced Blue-IRIS patterns. For both the tightly and loosely spaced Blue-IRIS patterns, five additional sections were analyzed for p-γ-H2AX/DAPI. In the case of femto-LASIK, a total of 24 sections were analyzed; 18 stained for TUNEL/DAPI and six for p-γ-H2AX/DAPI. In total, we counted over 42,000 cells from 234 images (see Fig. 3).

Cell counting was performed using custom software written in MATLAB (MathWorks, Natick, MA). A graphical user interface (GUI) was constructed that automatically counted

blue-(DAPI) and red- (TUNEL or p-γ-H2AX) stained cells in manually selected regions of interest (ROIs). To determine the distribution of TUNEL- or p-γ-H2AX-positive cells in and around the Blue-IRIS or femto-LASIK regions, these ROIs were first outlined (Fig. 3). The positions of the epithelium and the endothelium were then marked on each image, denoting the upper and lower bounds, respectively, of the corneal region to be analyzed. The program divided areas of the stroma above and below the ROIs into equally-spaced boxes, 25 μm tall. The custom software then used the "regionprops" function in MATLAB to define and count continuous objects (cells) and their centroids (centers of mass) separately for the red (TUNEL or p-γ-H2AX) and blue (DAPI) images. To reduce false positives generated from background noise, the "regionprops" function was used to determine the area of an average cell and exclude anything considered too small to be a cell. The ROI in Blue-IRIS treated corneas was defined as the area containing the closely or loosely spaced GRIN layers (Fig. 3A). For the femto-LASIK-treated corneas, the ROI encompassed the green auto-fluorescence that denoted the femtosecond laser-cut flap (Fig. 3B). The 4 mm region containing both the flap cut and the excimer laser ablation zone was identified by the presence of TUNEL-positive cells extending deeper into the stroma, well below the femto-flap, near the center of the cornea.

3 Results

3.1 TUNEL Staining

Blue-IRIS patterns were readily identifiable histologically from their green auto-fluorescence under 488 nm illumination (Figs. 3–5). TUNEL-positive cells were only evident in the stromal region of these corneas; the epithelium and endothelium were clear of TUNEL staining. Importantly, the endothelium stained positively for DAPI and appeared regular and intact across the entire cornea, both below areas where Blue-IRIS was performed and areas where no laser interaction occurred in the stroma. Within the stroma, TUNEL-positive cells were concentrated in regions of RI change. When the three Blue-IRIS layers were tightly spaced (10 μm or less), approximately 73% of keratocytes in the center of the laser-treated region became TUNEL-positive (Fig. 4A, B; Table 1). This percentage decreased as a function of distance away from the central Blue-IRIS layer (Figs. 4A, B) so that 44 μm away from the edge of the pattern, less than 10% of stromal cells were TUNEL-positive (Table 1) and no TUNEL-positive cells were ever seen >60 μm from the bottom of the ROI.

The precise location of TUNEL-positive cells relative to the Blue-IRIS focal zone was even more clearly defined when GRIN layers were widely separated (Fig. 4C): keratocytes between the layers remained largely TUNEL-negative, causing the overall percentage of TUNEL-positive keratocytes to peak around 53% in the ROI of the "loose" Blue-IRIS patterns (Figs. 4C, D; Table 1). At 22 μm from the edge of the "loose" Blue-IRIS patterns, less than 10% of stromal keratocytes were TUNEL-positive, and no TUNEL-positive cells were found >58 μm above, below or to the side of the edge of loose Blue-IRIS patterns (Table 1).

Femto-LASIK flap cuts were also easily identified by their green auto-fluorescence and concentration of TUNEL-positive cells (Figs. 3, 4E, 4G). About 50% of stromal keratocytes

in the flap cut were TUNEL-positive, decreasing to about 20% within the adjacent 50 μm of stroma outside of the 4 mm optical zone (Table 1). Stromal TUNEL-positive cells were observed to a depth of just over 100 μm below the flap cut. It should also be noted that TUNEL-positive epithelial cells were seen at the edge of the femtosecond flap cut, where the epithelium was cut. TUNEL-positive cells were seen across the entire 8.5 mm femto-flap, but extended more deeply into the stroma in the 4 mm area affected by the excimer laser photo-ablation. While corneal tissue in the central femto-LASIK-treated zone was ablated and thus, could not be included in our analyses, the sub-ablation zone contained many stromal cells that stained positive for TUNEL up to a depth of just over 150 μm below the flap cut (Figs. 4G, H). Thus, positive TUNEL staining occurred much deeper in the stroma of the sub-ablation zone in femto-LASIK-treated eyes than in flap-only regions, or Blue-IRIS-treated regions.

3.2 p-γ-H2AX staining

Antibody staining for p-γ-H2AX following Blue-IRIS was completely negative in the epithelium, endothelium and stroma aside from stromal areas directly *adjacent* to the GRIN layers. GRIN layer spacing did not appear to influence the overall percentage of p-γ-H2AX-positive cells inside the Blue-IRIS pattern ROIs or within 50 μm of the edge of these patterns (Table 2, Fig. 5A–D). In fact, the loose Blue-IRIS patterns allowed us to identify the most substantial difference between TUNEL and p-γ-H2AX staining: unlike TUNEL-positive cells, p-γ-H2AX-positive cells were precisely positioned directly *adjacent* to individual GRIN layers, rather than intersecting with them (Fig. 4A–D).

Femto-LASIK-treated corneas were entirely devoid of p-γ-H2AX staining, whether in the flap-only area, the sub-ablation zone, the epithelium, or the endothelium (Fig. 5E, F).

4 Discussion

The present study assessed cell damage caused by Blue-IRIS in the cornea, a new approach to laser refractive correction in which corneal tissue is neither removed nor cut. Instead, GRIN lenses are “written” directly into the corneal stroma using a low-pulse-energy, high-repetition-rate, femtosecond laser at 400 nm. While this regime is intended to work below the ablation threshold of the stromal “material” (cells + extracellular matrix), the important questions asked here were whether this process caused DNA damage in resident cells and in what distribution relative to the laser focal zone. To answer these questions, our experiments quantified the distribution of p-γ-H2AX- and TUNEL-positive cells in feline corneas 6 hrs after Blue-IRIS, contrasting it with staining patterns obtained 6 hrs after femto-LASIK, also in feline corneas.

4.1 Methodological considerations

While TUNEL staining is often used to detect dying cells (Gavrieli *et al.*, 1992), whether it labels apoptotic and/or necrotic cells is disputed (Gavrieli *et al.*, 1992; Wilson, 2000; Wilson *et al.*, 1996). As such, we make no claims about the exact mechanism of cell death resulting from Blue-IRIS or femto-LASIK. The significance of positive p-γ-H2AX immunostaining is also controversial: some studies suggest that increased p-γ-H2AX expression indicates

repairable double-stranded DNA breaks (Clingen *et al.*, 2008; Kuo and Yang, 2008; Mah *et al.*, 2010; Van Attikum and Gasser, 2009); others suggest that phosphorylation of γ-H2AX can occur in the absence of double-stranded DNA breaks, instead reflecting changes to chromatin structure (Baure *et al.*, 2009). In the cornea, Jester and colleagues showed that the anti-fibrotic drug Mitomycin C (MMC) induced p-γ-H2AX staining in stromal keratocytes; the authors suggested that phosphorylation of the histone H2AX was brought about by inter-strand crosslinking in the DNA (Jester *et al.*, 2012). MMC is highly toxic, blocking cell replication and altering gene transcription. Aside from killing a number of keratocytes, the appearance and persistence of p-γ-H2AX staining after MMC treatment of the cornea was suggested to indicate persistent DNA damage in surviving stromal keratocytes (Jester *et al.*, 2012). Baure and colleagues showed that altered osmolarity [in particular, hypotonicity] can also cause positive immunostaining for p-γ-H2AX in human fibroblasts as well as in neural precursor cells isolated from mouse cerebellum, positing that this results from altered chromatin structure in the absence of double-stranded breaks and without killing the cells (Baure *et al.*, 2009). Upon a return to isotonic conditions, p-γ-H2AX staining first stayed constant, then increased after 2 hours, suggesting that increased p-γ-H2AX expression was due to *changes* in osmolarity. In sum, recent evidence shows up-regulated phosphorylation of γ-H2AX, both in cases of DNA damage and when there are changes in chromatin structure without damage or death (Baure *et al.*, 2009). Thus, p-γ-H2AX could be considered a global marker of histone modification and signal transduction in DNA damage/repair responses (Clingen *et al.*, 2008; Kuo and Yang, 2008; Van Attikum and Gasser, 2009).

4.2 Characterizing the damage induced by Blue-IRIS

While Blue-IRIS involves no tissue removal (which means that a large population of keratocytes is preserved), we observed TUNEL-positive cells where Blue-IRIS layers crossed stromal keratocytes. This suggests that a portion of the cells directly in the path of the laser focal spot were sufficiently damaged to eventually induce death. If Blue-IRIS layers were separated by 30 μm, fewer cells died than if the layers were close together, suggesting potentiation of the effect by proximity of laser focal zones to each other.

Curiously, cells *adjacent* to Blue-IRIS focal spots were mostly positive for p-γ-H2AX rather than TUNEL. Possible explanations for this observation include: (1) while not within the laser focal zone, adjacent keratocytes were still close enough to receive energy deposition (perhaps in the form of thermal accumulation) sufficient for DNA damage; (2) dying (TUNEL-positive) keratocytes inside Blue-IRIS layers communicated a ‘death signal’ to surrounding keratocytes via gap junctions (Grupcheva *et al.*, 2012; Jester *et al.*, 1995; Spanakis *et al.*, 1998; Ueda *et al.*, 1987; Watsky, 1995); (3) Blue-IRIS lines were associated with localized changes in osmolarity. Consistent with this third option, our prior work in hydrogels showed that water removal from the laser focal area into the surrounding material was likely responsible for the observed change in refractive index (Ding *et al.*, 2006). In cornea, a similar process could lead to localized “densification” of the extracellular matrix in the laser focal zone (and an increase in RI), together with water displacement away from this zone. Therefore, areas adjacent to the GRIN lines may experience a localized decrease in osmolarity and this, rather than permanent DNA damage or double-stranded breaks, could underlie the increased expression of p-γ-H2AX in near-Blue-IRIS keratocytes.

4.3 Comparing cell damage in Blue-IRIS and femto-LASIK

TUNEL-and p-γ-H2AX-positive cells were largely restricted to the Blue-IRIS patterns and neighboring stromal keratocytes. In the ~500 μm thick cat corneas used here, they never extended more than ~75 μm from the center of Blue-IRIS patterns in any direction (Table 1). This is likely because outside the Blue-IRIS focal zones, the incident irradiation was insufficient to generate the non-linear interactions necessary to cause RI change or cell damage. Notably, while Blue-IRIS only employs a 400 nm femtosecond laser operating below the damage threshold of cornea, femto-LASIK utilizes a femtosecond laser for epithelial flap creation and an excimer laser for photo-ablation of the stromal bed. Because the diameter of the femto-flap was 8.5 mm, while the excimer OZ was restricted to the central 4 mm of exposed stromal bed, we were able to dissociate the relative impact of the two laser ablations. TUNEL-staining was seen along the entire femto-flap, not just in the sub-excimer ablation area, indicating both lasers used in femto-LASIK induce cell death in the cornea.

One limitation in our attempt to compare femto-LASIK and Blue-IRIS was that the optical zones were not perfectly matched - the 2.5 mm IRIS patterns were the largest we could generate with our apparatus; 4 mm was the smallest OZ diameter permitted by the Technolas laser algorithm. As such, there was a size disparity between stromal areas affected by the excimer laser ablation (LASIK) and IRIS. TUNEL staining extended more deeply into the stroma in the 4 mm OZ than in the flap-only region and the staining extended deeper than that seen adjacent to IRIS patterns. We cannot – at this stage – discriminate whether the extended depth of TUNEL-staining in femto-LASIK resulted from the cumulative effect of femto flap cutting and excimer ablation, or the larger OZ size. Nonetheless, it appears that TUNEL staining was generally less prevalent and more localized in IRIS-treated corneas than in LASIK-treated ones.

In addition to Blue-IRIS being advantageous for minimizing cell death in the stroma, epithelial and endothelial cell health also appeared unaffected by the Blue-IRIS procedure. Femto-LASIK exhibited additional damage from the flap cutting process, which involved not only the stroma, but also the epithelium at the edges of the flap. These cells, plus the stromal cells that were ablated, and the stromal keratocytes that turned TUNEL-positive past a depth of 150 μm below the ablation zone, all suggest that overall, Blue-IRIS causes markedly less cell death and damage than femto-LASIK when used to achieve a similar change in ocular refraction.

4.4 Conclusions

After performing femto-LASIK and Blue-IRIS in feline corneas, TUNEL staining suggests that significantly less cell death occurs in the cornea following Blue-IRIS treatment. In addition, an interesting observation emerged from p-γ-H2AX staining, which was completely absent after femto-LASIK, but present adjacent to Blue-IRIS GRIN lines. While DNA damage caused by energy deposition or a death signal from TUNEL-positive keratocytes cannot be completely ruled out, ongoing investigations are now assessing a potential role of water displacement – both as an explanation for p-γ-H2AX staining and a potential mechanism underlying the RI change in Blue-IRIS.

Acknowledgments

The authors wish to thank Margaret DeMagistris for outstanding technical assistance during surgeries and post-operative tissue dissection, Tracy Bubel for tissue processing, corneal sectioning and photo-microscopy, Thurma McDaniel for performing TUNEL staining and immuno-histochemistry on corneal sections, and Dr. Douglas H. Kelley for MATLAB support. This project was supported by an unrestricted grant to the University of Rochester's Department of Ophthalmology from the Research to Prevent Blindness (RPB) Foundation, by the National Institutes of Health (R01 grant EY015836 to KRH; Core grant P30 EY01319F to the Center for Visual Science; a Center for Visual Science training grant fellowship T32 EY007125 to DES), by a grant from Clerio Vision, Inc. with matching funds from the University of Rochester's Center for Emerging & Innovative Sciences, a NYSTAR-designated Center for Advanced Technology, and by an Incubator Grant from the University of Rochester's CTSI Scientific Advisory Committee (SAC).

Abbreviations

D	diopter
IRIS	intra-tissue refractive index shaping
LASIK	laser in-situ keratomileusis
RI	refractive index
NA	numerical aperture
GRIN	gradient index
TUNEL	terminal deoxynucleotidyl transferase-mediated dUTP-digoxigenin nick end labeling
p-γ-H2AX	phosphorylated form of γ-H2AX
GUI	graphical user interface
ROI	region of interest
ND	neutral density
MMC	Mitomycin C

References

Ambrósio R Jr, Tervo T, Wilson SE. LASIK-associated dry eye and neurotrophic epitheliopathy: pathophysiology and strategies for prevention and treatment. Journal of refractive surgery. 2008; 24(4):396–407. [PubMed: 18500091]

Baure J, Izadi A, Suarez V, Giedzinski E, Cleaver JE, Fike JR, Limoli CL. Histone H2AX phosphorylation in response to changes in chromatin structure induced by altered osmolarity. Mutagenesis. 2009; 24:161–167. [PubMed: 19064695]

Brooks DR, Brown NS, Savage DE, Wang C, Knox WH, Ellis JD. Precision large field scanning system for high numerical aperture lenses and application to femtosecond micromachining of ophthalmic materials. Review of Scientific Instruments. 2014; 85:065107. [PubMed: 24985852]

Campos M, Szerenyi K, Lee M, McDonnell JM, Lopez PF, McDonnell PJ. Keratocyte loss after corneal deepithelialization in primates and rabbits. Archives of ophthalmology. 1994; 112:254–260. [PubMed: 8311779]

Clingen P, Wu J-H, Miller J, Mistry N, Chin F, Wynne P, Prise K, Hartley J. Histone H2AX phosphorylation as a molecular pharmacological marker for DNA interstrand crosslink cancer chemotherapy. Biochemical pharmacology. 2008; 76:19–27. [PubMed: 18508035]

Ding L, Blackwell R, Kunzler JF, Knox WH. Large refractive index change in silicone-based and non-silicone-based hydrogel polymers induced by femtosecond laser micro-machining. Optics express. 2006; 14:11901–11909. [PubMed: 19529613]

Ding L, Cancado LG, Novotny L, Knox WH, Anderson N, Jani D, Linhardt J, Blackwell RI, Künzler JF. Micro-Raman spectroscopy of refractive index microstructures in silicone-based hydrogel polymers created by high-repetition-rate femtosecond laser micromachining. JOSA B. 2009; 26:595–602.

Ding L, Knox WH, Bühren J, Nagy LJ, Huxlin KR. Intra-tissue Refractive Index Shaping (IRIS) of the cornea and lens using a low-pulse-energy femtosecond laser oscillator. Investigative ophthalmology & visual science. 2008; 49:5332. [PubMed: 18641284]

Fan-Paul NI, Li J, Miller JS, Florakis GJ. Night vision disturbances after corneal refractive surgery. Survey of ophthalmology. 2002; 47:533–546. [PubMed: 12504738]

Gavrieli Y, Sherman Y, Ben-Sasson SA. Identification of programmed cell death in situ via specific labeling of nuclear DNA fragmentation. The Journal of cell biology. 1992; 119:493–501. [PubMed: 1400587]

Grupcheva CN, Laux WT, Rupenthal ID, McGhee J, McGhee C, Green CR. Improved corneal wound healing through modulation of gap junction communication using connexin43-specific antisense oligodeoxynucleotides. Invest Ophthalmol Vis Sci. 2012; 53:1130–1138. [PubMed: 22247467]

Helena MC, Baerveldt F, Kim W-J, Wilson SE. Keratocyte apoptosis after corneal surgery. Investigative Ophthalmology and Visual Science. 1998; 39:276–283. [PubMed: 9477983]

Jester JV, Nien CJ, Vasiliou V, Brown DJ. Quiescent keratocytes fail to repair MMC induced DNA damage leading to the long-term inhibition of myofibroblast differentiation and wound healing. Molecular vision. 2012; 18:1828. [PubMed: 22815636]

Jester JV, Petroll WM, Barry PA, Cavanagh HD. Temporal, 3-dimensional, cellular anatomy of corneal wound tissue. Journal of anatomy. 1995; 186:301. [PubMed: 7649828]

Kuo LJ, Yang L-X. γ-H2AX-a novel biomarker for DNA double-strand breaks. In Vivo. 2008; 22:305–309. [PubMed: 18610740]

Mah L, El-Osta A, Karagiannis T. γH2AX: a sensitive molecular marker of DNA damage and repair. Leukemia. 2010; 24:679–686. [PubMed: 20130602]

Meltendorf C, Burbach GJ, Bühren J, Bug R, Ohrloff C, Deller T. Corneal femtosecond laser keratotomy results in isolated stromal injury and favorable wound-healing response. Investigative ophthalmology & visual science. 2007; 48:2068–2075. [PubMed: 17460262]

Mohan RR, Hutcheon AE, Choi R, Hong J, Lee J, Mohan RR, Ambrósio R, Zieske JD, Wilson SE. Apoptosis, necrosis, proliferation, and myofibroblast generation in the stroma following LASIK and PRK. Experimental eye research. 2003; 76:71–87. [PubMed: 12589777]

Møller-Pedersen T, Cavanagh HD, Petroll WM, Jester JV. Stromal wound healing explains refractive instability and haze development after photorefractive keratectomy: a 1-year confocal microscopic study. Ophthalmology. 2000; 107:1235–1245. [PubMed: 10889092]

Nagy LJ, Ding L, Xu L, Knox WH, Huxlin KR. Potentiation of femtosecond laser intratissue refractive index shaping (IRIS) in the living cornea with sodium fluorescein. Investigative ophthalmology & visual science. 2010; 51:850. [PubMed: 19815735]

Nakamura K, Kurosaka D, Bissen-Miyajima H, Tsubota K. Intact corneal epithelium is essential for the prevention of stromal haze after laser assisted in situ keratomileusis. British journal of ophthalmology. 2001; 85:209–213. [PubMed: 11159488]

Netto MV, Mohan RR, Ambrósio R Jr, Hutcheon AE, Zieske JD, Wilson SE. Wound healing in the cornea: a review of refractive surgery complications and new prospects for therapy. Cornea. 2005; 24:509–522. [PubMed: 15968154]

Netto MV, Mohan RR, Medeiros FW, Dupps WJ Jr, Sinha S, Krueger RR, Stapleton WM, Rayborn M, Suto C, Wilson SE. Femtosecond laser and microkeratome corneal flaps: comparison of stromal wound healing and inflammation. Journal of refractive surgery (Thorofare, NJ: 1995). 2007; 23:667.

Savage DE, Brooks DR, DeMagistris M, Xu L, MacRae S, Ellis JD, Knox WH, Huxlin KR. First demonstration of ocular refractive change using blue-iris in live cats. Investigative ophthalmology & visual science. 2014; 55:4603. [PubMed: 24985471]

Spanakis SG, Petridou S, Masur SK. Functional gap junctions in corneal fibroblasts and myofibroblasts. Investigative ophthalmology & visual science. 1998; 39:1320–1328. [PubMed: 9660479]

Ueda A, Nishida T, Otori T, Fujita H. Electron-microscopic studies on the presence of gap junctions between corneal fibroblasts in rabbits. Cell and tissue research. 1987; 249:473–475. [PubMed: 3621310]

Van Attikum H, Gasser SM. Crosstalk between histone modifications during the DNA damage response. Trends in cell biology. 2009; 19:207–217. [PubMed: 19342239]

Vogel A, Noack J, Hüttman G, Paltauf G. Mechanisms of femtosecond laser nanosurgery of cells and tissues. Applied Physics B. 2005; 81:1015–1047.

Watsky MA. Keratocyte gap junctional communication in normal and wounded rabbit corneas and human corneas. Investigative ophthalmology & visual science. 1995; 36:2568–2576. [PubMed: 7499079]

Wilson SE. Molecular cell biology for the refractive corneal surgeon: programmed cell death and wound healing. Journal of Refractive Surgery. 1997; 13:171. [PubMed: 9109075]

Wilson SE. Role of apoptosis in wound healing in the cornea. Cornea. 2000; 19:S7–S12. [PubMed: 10832715]

Wilson SE, He Y-G, Weng J, Li Q, McDowall AW, Vital M, Chwang EL. Epithelial injury induces keratocyte apoptosis: hypothesized role for the interleukin-1 system in the modulation of corneal tissue organization and wound healing. Experimental eye research. 1996; 62:325–338. [PubMed: 8795451]

Wilson SE, Kim W-J. Keratocyte apoptosis: implications on corneal wound healing, tissue organization, and disease. Investigative Ophthalmology and Visual Science. 1998; 39:220–226. [PubMed: 9477978]

Xu L, Huxlin KR, DeMagistris M, Wang N, Ding L, Knox WH. Non-invasive Blue Intra-tissue Refractive Index Shaping (IRIS) in Living, Excised Cornea, Frontiers in Optics. Optical Society of America. 2010:PDPA11.

Xu L, Knox WH, DeMagistris M, Wang N, Huxlin KR. Noninvasive intratissue refractive index shaping (IRIS) of the cornea with blue femtosecond laser light. Investigative ophthalmology & visual science. 2011a; 52:8148. [PubMed: 21931133]

Xu L, Knox WH, Huxlin KR. Exogenous and endogenous two-photon absorption for Intra-tissue Refractive Index Shaping (IRIS) in live corneal tissue [Invited]. Optical Materials Express. 2011b; 1:1159–1164.

Highlights

- Blue-IRIS alters the refractive index of corneal tissue
- Blue-IRIS is non-invasive; the epithelium and endothelium remain intact
- Cell damage is minimal and more localized in IRIS than femto-LASIK
- DNA damage occurs in laser focal zones
- Localized osmolarity changes may underlie corneal refractive index change

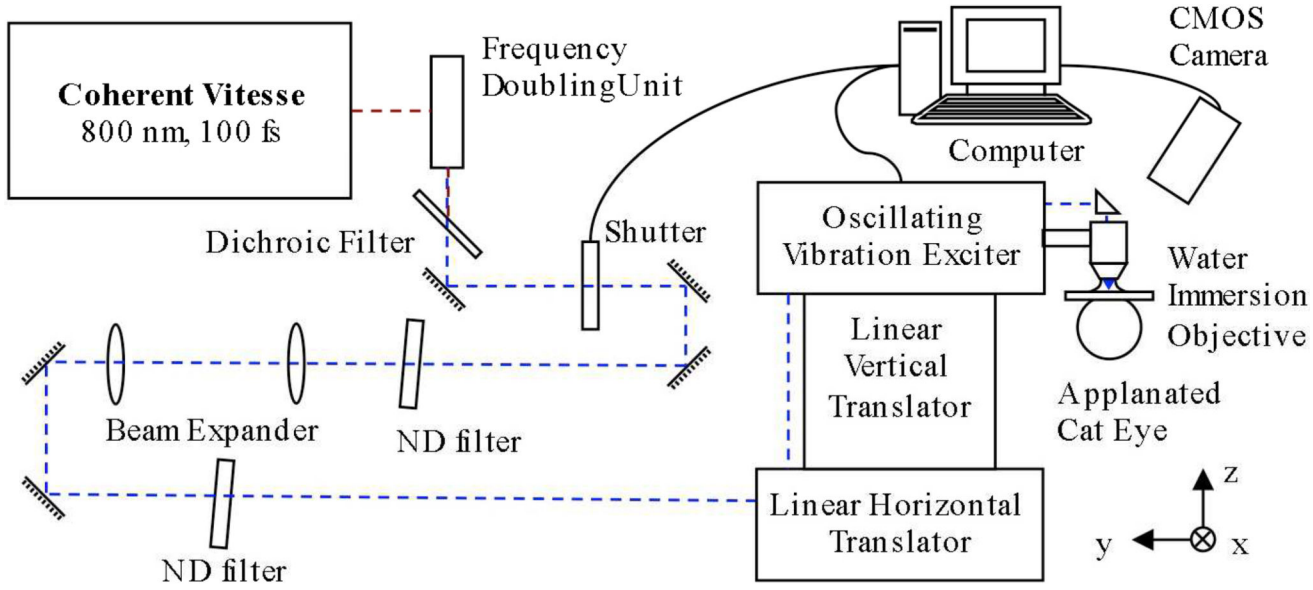

Figure 1. Blue-IRIS apparatus

An 800 nm, 100 fs Coherent Vitesse laser beam was frequency doubled to produce 400 nm laser pulses, which were tightly focused through a 1.0 NA, water immersion objective, into the stromal layer of applanated feline corneas. A complementary metal-oxide semiconductor (CMOS) camera was used to find the interface between the applanator and cornea, thus locating the surface of the enucleated globe. The objective was then lowered such that the focal spot was located in the mid stromal region. A commercial, oscillating, vibration exciter was used in combination with a linear translation stage to raster-scan across a 2.5 mm × 2.5 mm area in the center of each cornea. ND filter: neutral density filter.

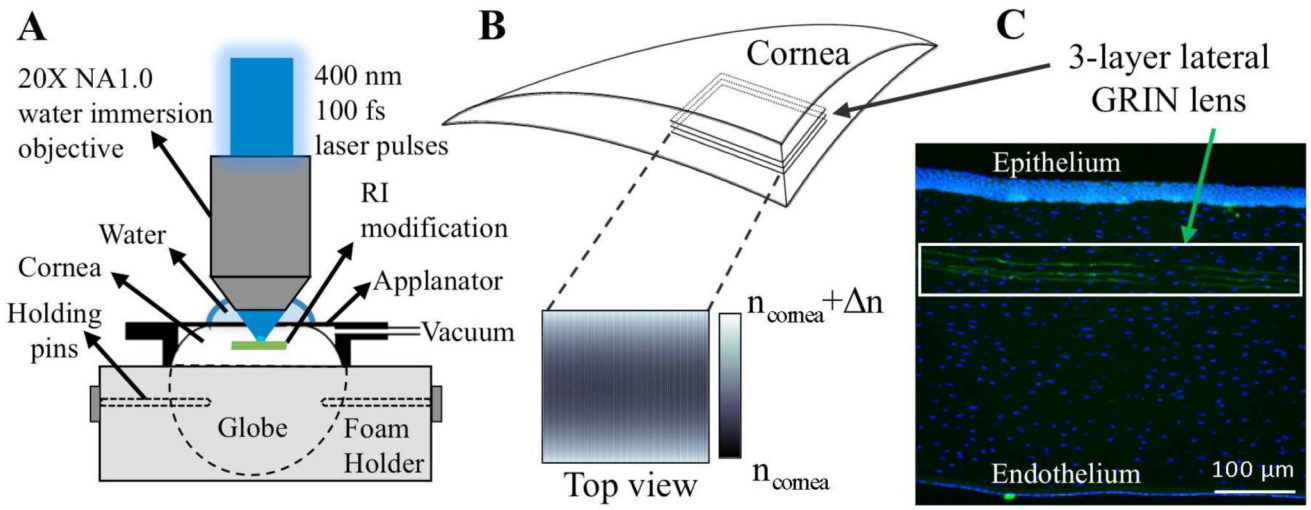

Figure 2. Blue-IRIS in excised cat cornea

A. The focal region of the objective was scanned through the cornea using 3-axis delivery system to inscribe a cylindrical GRIN lens. **B**. Schematic of a corneal segment containing an inscribed, mid-stromal, 3-layer GRIN pattern. A top-view, schematic representation of the refractive index change distribution induced by the femtosecond laser across a single Blue-IRIS GRIN layer is shown below the corneal segment. **C**. Photomicrograph of the entire stroma (epithelium to endothelium), containing a 3-layer Blue-IRIS pattern (green auto-fluorescence). The tissue was counterstained with DAPI (blue fluorescence).

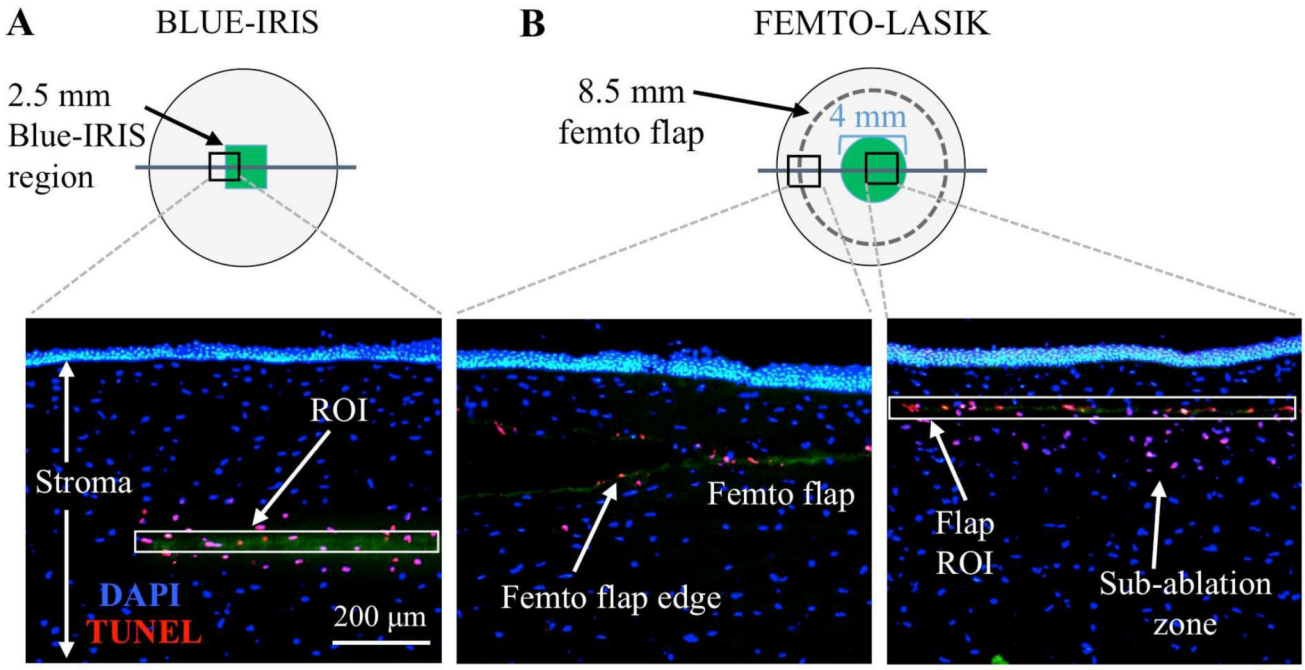

Figure 3. Method for quantitative analysis of TUNEL/p-γ-H2AX staining in sectioned corneas

Magnification is the same for all photomicrographs. **A** and **B** show en-face, schematics of corneas with the approximate size and positioning of Blue-IRIS and femto-LASIK procedures respectively. The straight line through each schematic cornea illustrates approximate source of the putative cross-section, with typical staining patterns (in this case, TUNEL/DAPI) imaged in the photomicrographs below each schematic. **A**. In Blue-IRIS-treated cornea, the region of interest (ROI) was set to encompass the lateral edge of the GRIN lens (green auto-fluorescence). **B**. The ROI in the two femto-LASIK-treated corneal sections encompassed the edge of the femtosecond flap (green auto-fluorescence) and the femto-flap + sub-ablation zone, which was recognized because it possessed an additional region of TUNEL-positive cells extending into the stroma, below the flap, in the approximate center of the cornea.

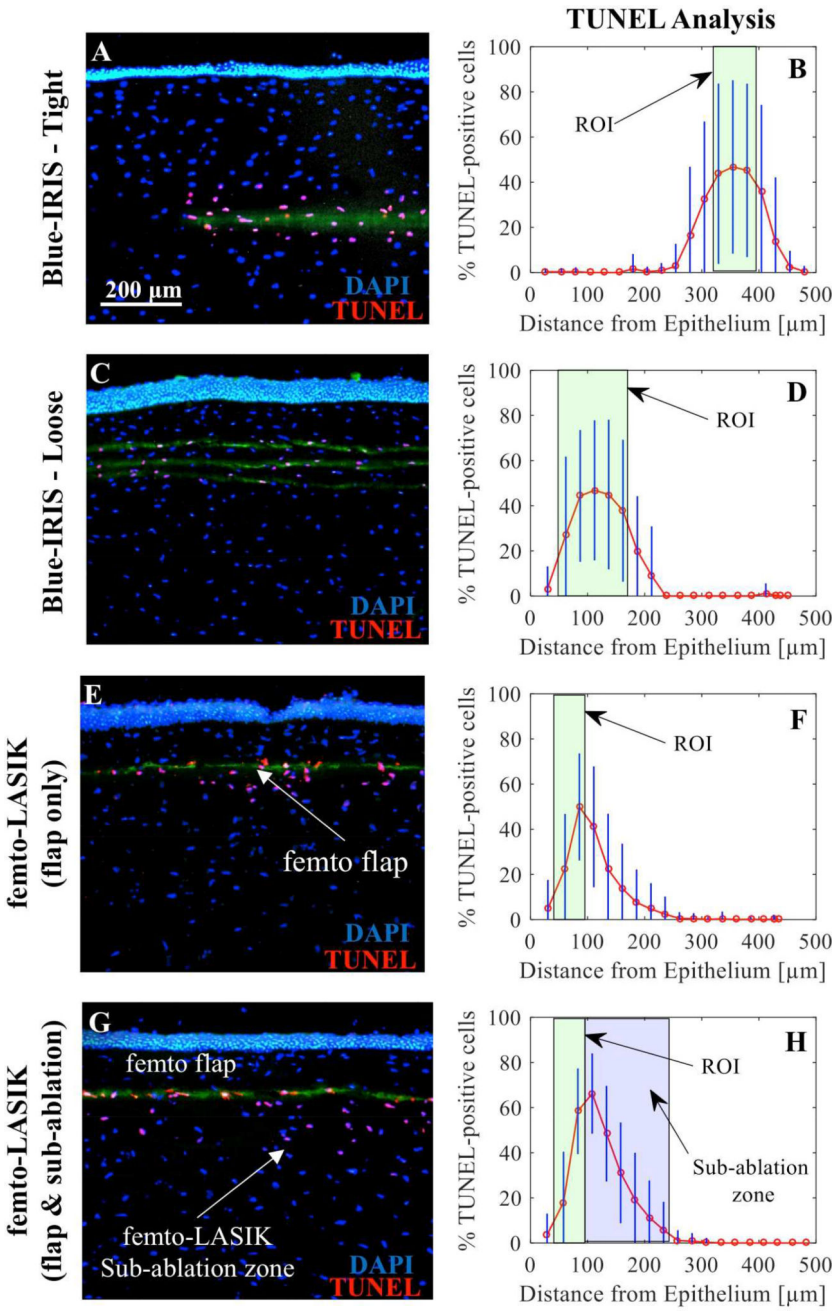

Figure 4. TUNEL assay in Blue-IRIS-and femto-LASIK-treated feline corneas

In all photomicrographs (**A, C, E, G**), green auto-fluorescence indicates areas of Blue-IRIS or flap cut for femto-LASIK-treated corneas. Red/pink staining indicates TUNEL-positive cells. Blue fluorescence denotes DAPI-positive cell nuclei. Corneal sections are oriented with the epithelium uppermost. Magnification is identical in all photomicrographs. All graphs (**B, D, F, H**) plot the percentage (%) of DAPI-positive cells also positive for TUNEL, as a function of distance from the epithelial-stromal interface. The overlaid green area shows size and position of each ROI relative to the epithelium; the overlaid blue box in **H** indicates the size and position of the sub-ablation zone.

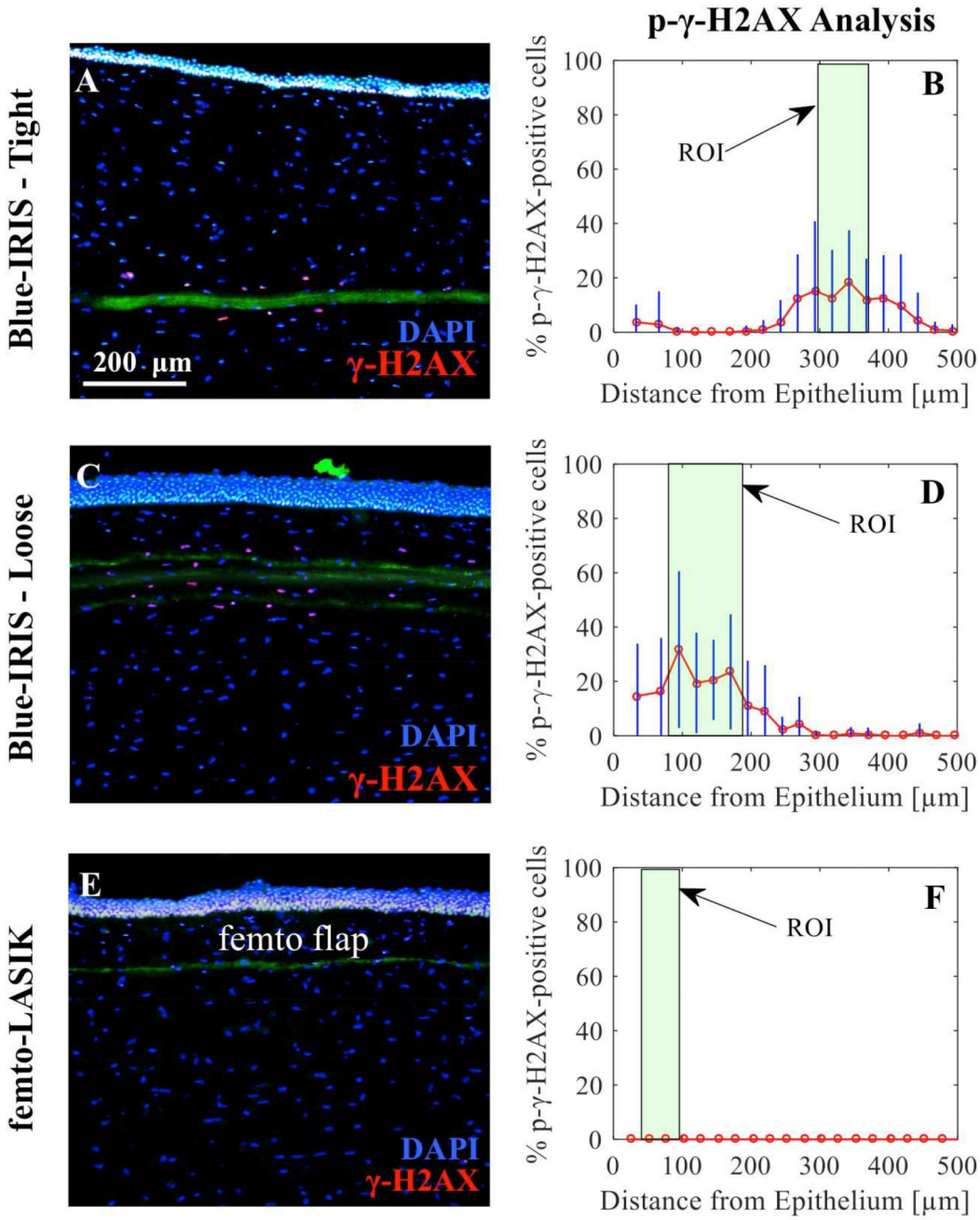

Figure 5. p-γ-H2AX antibody staining for Blue-IRIS-and femto-LASIK-treated feline corneas

Photomicrographs in **A, C, E**, show stained corneal sections with green auto-fluorescence denoting areas of Blue-IRIS or flap cut for femto-LASIK-treated corneas, red/pink indicating p-γ-H2AX-positive cells and blue denoting DAPI-positive cell nuclei. Corneal sections are oriented with the epithelium uppermost. Magnification is identical in all photomicrographs. Adjacent graphs (**B, D, F**) plot the percentage (%) of DAPI-labeled cells positive for p-γ-H2AX, as a function of distance from the epithelial-stromal interface. The

overlaid green boxes inside each graph shows the approximate size and position of each ROI relative to the epithelium.

Table 1

Concentration and distribution of TUNEL-positive cells in different regions of interest (ROIs) of corneas treated with Blue-IRIS or femto-LASIK.

	Blue-IRIS Tight*	Blue-IRIS Loose*	femto-LASIK Flap	femto-LASIK Sub-ablation
TUNEL positive cells in ROI (% total cells)	73 ± 16	53 ± 7	50 ± 14	50 ± 14
TUNEL positive cells ±50 μm from ROI (% total cells)	9 ± 17	2 ± 5	22 ± 25	36 ± 24
Max. depth for TUNEL positive cells (μm from center of the ROI)	56	58	>100	>150
Distance from ROI where TUNEL positive cells ≈ 10% (μm from edge of ROI)	44	22	78	125

*Tight and loose refer to the spacing of GRIN layers in Blue-IRIS treated corneas.

Values are means ± SD where warranted.

Table 2

Concentration and distribution of p-γ-H2AX-positive cells in different regions of interest (ROIs) of corneas treated with Blue-IRIS.

	Blue-IRIS Tight*	Blue-IRIS Loose*
p-γ-H2AX positive cells in ROI (% total cells)	16 ± 8	24 ± 10
p-γ-H2AX positive cells ±50 μm from ROI (% total cells)	13 ± 18	8 ± 12
Max. depth for p-γ-H2AX positive cells (μm from center of the ROI)	69	75
Distance from ROI where p-γ-H2AX positive cells ≈ 10% (μm from edge of ROI)	63	34

*Tight and loose refer to the spacing of GRIN layers in Blue-IRIS treated corneas.

Values are means ± SD where warranted.